Spatial evolution of short laser pulses under coherent population trapping

V. G. Arkhipkin
Institute of Physics, Russian Academy of Sciences, 660036 Krasnoyarsk, Russia and Krasnoyarsk State Technical University, 660074 Krasnoyarsk, Russia

I. V. Timofeev
Krasnoyarsk State University, 660041 Krasnoyarsk Street, Svobodny, 79, Russia
(Received 21 March 2001; published 12 October 2001)

The spatial and temporal evolution is studied of two powerful short laser pulses having different wavelengths and interacting with a dense three-level Λ-type optical medium under coherent population trapping. The general case of unequal oscillator strengths of the transitions is considered. The durations of the probe pulse and the coupling pulse $T_{1,2}$ $(T_2 > T_1)$ are assumed to be shorter than any of the relevant atomic relaxation times. We propose analytical and numerical solutions of a self-consistent set of coupled Schrödinger equations and reduced wave equations in the adiabatic limit taking account of the first nonadiabatic correction. The adiabaticity criterion is also discussed taking account of pulse propagation. The dynamics of propagation is found to be strongly dependent on the ratio of the transition oscillator strengths. It is shown that the envelopes of the pulses slightly change throughout the medium length in the initial stage of propagation. This distance can be large compared to the one-photon resonant absorption length. Eventually, the probe pulse is completely reemitted into the coupling pulse during propagation. An effect of localization of the atomic coherence was observed similar to the one predicted by Fleischhauer and Lukin [Phys. Rev. Lett. **84**, 5094 (2000)].

DOI: 10.1103/PhysRevA.64.053811 PACS number(s): 42.50.Gy, 42.50.Hz, 42.65.Tg

I. INTRODUCTION

Electromagnetically induced transparency (EIT) can be used to make optically thick media transparent to resonant laser radiation [1]. The EIT is the result of various quantum interference effects such as nonlinear interference [2], coherent population trapping (CPT) [3,4], and adiabatic population transfer (APT) [5]. The optical characteristics of the matter undergo drastic changes under those effects to such an extent that they can now be manipulated. A lot of interesting applications based on that have been proposed and experimentally realized (see, e.g., [3–10]).

Interesting and unusual phenomena caused by the above indicated effects can be observed when laser pulses propagate in a resonant three-level medium. The propagation of pulses under EIT conditions was studied, for example, in [11–18]. As a rule, situations are considered when both pulses have identical forms and their duration is longer than the relaxation time of the intermediate resonant state (matched pulses [11]; dressed field pulses [12,13]) or when the duration of the coupling radiation considerably exceeds that of the probe radiation (adiabatons [15,16,19]). A theoretical study of certain features of spatial evolution under APT conditions is presented in [16,17,20]. Propagation of solitonlike pulses in a three-level system is studied in [21]. A three-level system with equal oscillator strengths is considered in all the above mentioned studies, whereas in actual fact the transition oscillator strengths are most often different.

In this paper, the spatial and temporal evolution is studied of two overlapping short laser pulses propagating in a resonant optically thick medium that consists of three-level Λ atoms. Pulses of such configuration are widely used to enhance the efficiency of nonlinear generation processes [22,23]. The two pulses are assumed to have identical shapes but different durations $(T_2 > T_1)$ as shown in Fig. 1. The pulse durations are much shorter than any of the times of relaxation in the medium (short pulses). It is also assumed that the pulse envelopes satisfy the adiabaticity criterion [13,24,25]

$$(G_2 \dot{G}_1 - G_1 \dot{G}_2)/G^3 \ll 1, \tag{1}$$

where $G_{1,2}$ are the Rabi frequencies of the respective fields, $G = \sqrt{G_1^2 + G_2^2}$; the overdot refers to time derivatives. Condition (1) is easy to satisfy by making one of the pulse amplitudes or both of them large even for short pulses. This will induce strong coherence at the Raman transition resulting in the effect of CPT. The latter considerably decreases the absorption of the propagating resonant pulses. The dynamics of propagation of such pulses is studied here without restriction of the relationship between the oscillator strengths of the transitions.

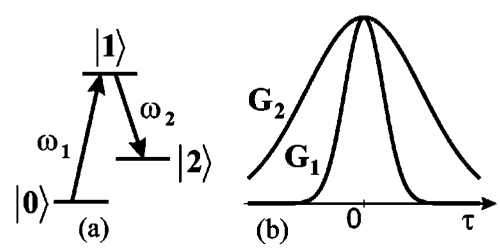

FIG. 1. (a) The three-level Λ-type system coupled by two resonant pulses with Rabi frequencies G_1 and G_2. (b) The shapes of probe G_1 and coupling G_2 pulses at the medium entrance.

Our theoretical model involves a set of coupled Schrödinger equations and a set of reduced wave equations, allowing thus a simultaneous description of temporal and spatial evolution of the atomic system and the radiation. The equations are analyzed in approximation (1) taking account of the first nonadiabatic correction. It will be shown that the dynamics of propagation strongly depends on the oscillator strength ratio. Also analyzed is the spatial and temporal behavior of the atomic Raman coherence. The possibility of localizing the atomic coherence spatially has been established. The results obtained are compared to the results reported in [26].

The paper is organized as follows. In Sec. II, we describe the model and present the basic equations. Section III contains self-consistent solutions of those equations in the adiabatic limit and describes the temporal behavior of the level populations and the atomic Raman coherence in an optically thin medium. The spatial evolution of pulses in an optically thick medium is described in Sec. IV for various oscillator strength ratios. In Sec. IV, we also discuss the adiabaticity criterion and demonstrate the effect of spatial localization of the atomic coherence. Finally, we summarize the results obtained.

II. BASIC EQUATIONS

The three-level system under consideration is shown in Fig. 1 together with the temporal configuration of the pulses as they enter the medium. The pulses travel along the same direction z. States $|0\rangle$, $|1\rangle$, and $|2\rangle$ are connected by laser pulses $E_1 = 1/2E_1(t)\exp[-i(\omega_1 t - k_1 z)] + \text{c.c.}$ and $E_2 = 1/2E_2(t)\exp[-i(\omega_2 t - k_2 z)] + \text{c.c.}$, respectively. In our further consideration we shall refer to the first pulse E_1 as the probe and to the second pulse E_2 as the coupling pulse. The Rabi frequency of the probe pulse is comparable with that of the coupling pulse. The pulses are sent simultaneously into an atom. The pulse durations $T_{1,2}$ ($T_2 > T_1$) are assumed to be much less than any of the relaxation times of atoms. The transition $|0\rangle$-$|2\rangle$ is electric dipole forbidden. The intermediate state $|1\rangle$ is in one-photon resonance with each field, interacting only with the corresponding transition.

The following standard set of equations describes the spatial and temporal dynamics of the probability amplitudes of atomic states $b_{0,1,2}$ and slowly varying Rabi frequencies $G_1 = d_{10}E_1(t)/2\hbar$, $G_2 = d_{21}E_2(t)/2\hbar$ in the local-time coordinate system $\tau = t - z/c$:

$$\frac{\partial b_0}{\partial \tau} = iG_1^* b_1 \exp(-ik_1 z),$$

$$\frac{\partial b_2}{\partial \tau} = iG_2^* b_1 \exp(-ik_2 z), \tag{2}$$

$$\frac{\partial b_1}{\partial \tau} = iG_1 b_0 \exp(ik_1 z) + iG_2 b_2 \exp(ik_2 z),$$

$$\frac{\partial G_1}{\partial z} = iK_1 b_1 b_0^* \exp(ik_1 z),$$

$$\frac{\partial G_2}{\partial z} = iK_2 b_1 b_2^* \exp(ik_2 z). \tag{3}$$

Here we assumed zero one-photon detunings. $K_{1,2} = \pi\omega_1 |d_{10,12}|^2 N/\hbar c$ are the propagation coefficients, N is the atomic concentration, $d_{10,12}$ are the dipole transition matrix elements, $\omega_{1,2}$ and $k_{1,2}$ are the frequencies and wave numbers of the interacting waves in vacuum, and c is the light velocity in vacuum. All atoms are assumed to be initially in the ground state $|0\rangle$: $b_0(-\infty, z) = 1$, $b_{1,2}(-\infty, z) = 0$. We use Gaussian pulses at the medium entrance $z = 0$ for the purpose of numerical simulation: $G_1(\tau) = G_1^0 \exp(-\tau^2 \ln 2/T_1^2)$, $G_2(\tau) = G_2^0 \exp[-\tau^2 \ln 2/T_2^2]$.

In terms of $a_0 = b_0 \exp(ik_1 z)$, $a_2 = b_2 \exp(ik_2 z)$, $a_1 = ib_1$, Eqs. (2) and (3) can be written as

$$\frac{\partial a_0}{\partial \tau} = G_1^* a_1,$$

$$\frac{\partial a_2}{\partial \tau} = G_2^* a_1, \tag{4}$$

$$\frac{\partial a_1}{\partial \tau} = -G_1 a_0 - G_2 a_2,$$

$$\frac{\partial G_1}{\partial z} = -K_1 a_1 a_0^*,$$

$$\frac{\partial G_2}{\partial z} = -K_2 a_1 a_2^*. \tag{5}$$

The coupled equations (4) and (5) give a complete semiclassical description of the resonant different-wavelength propagation problem we are dealing with.

III. TEMPORAL DYNAMICS OF LEVEL POPULATIONS AND RAMAN COHERENCE IN THE ADIABATIC APPROXIMATION (OPTICALLY THIN MEDIUM)

In this section we study the temporal dynamics of populations and the atomic coherence in the given time-dependent field, assuming that the medium is optically thin. Based on that, $G_{1,2}$ will not depend on the coordinate z. One can show that condition (1) for Gaussian pulses reduces to $G_2^0 T_1 \gg 1$ when $T_2/T_1 > \sqrt{2}$. With the first nonadiabatic correction, the solution of Eq. (4) takes the form

$$a_0 \simeq \frac{G_2(\tau)}{G(\tau)}, \quad a_2 \simeq -\frac{G_1(\tau)}{G(\tau)},$$

$$a_1 \simeq \frac{1}{G_1}\frac{\partial(G_2/G)}{\partial \tau} \simeq -\frac{1}{G_2}\frac{\partial(G_1/G)}{\partial \tau}, \tag{6}$$

where $G(\tau) = \sqrt{G_1^2(\tau) + G_2^2(\tau)}$.

The solutions for the probability amplitudes are conveniently represented as

$$a_0 = \cos\theta(\tau), \quad a_2 = -\sin\theta(\tau), \tag{7}$$

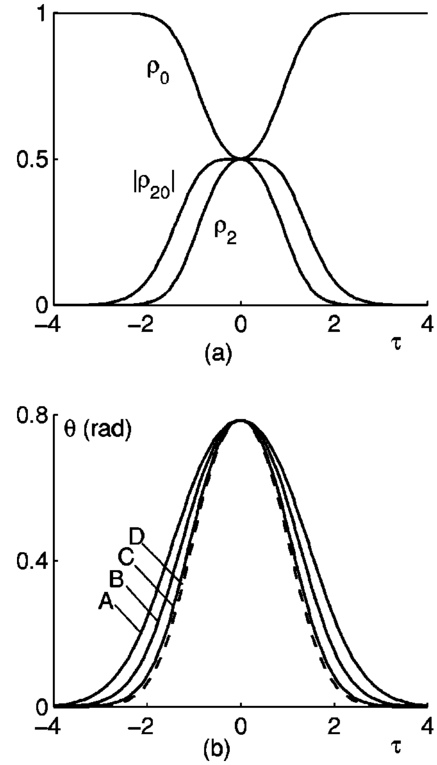

FIG. 2. The time evolution of (a) level populations $|a_{0,2}(\tau)|^2$ and the atomic Raman coherence $|\rho_{20}(\tau)|$; (b) the mixing angle $\theta(\tau)$ in an optically thin medium for the Gaussian pulses. $G_1^0 T_1 = G_2^0 T_1 = 20$, (a) $T_2/T_1 = 3$; (b) $T_2/T_1 = \sqrt{2}$ (A), $\sqrt{3}$ (B), 3 (C), 10 (D).

where the mixing angle $\theta(\tau)$ is defined as $\tan\theta(\tau) = G_1(\tau)/G_2(\tau)$ (we shall discuss its meaning later on).

The expression for a_1 can be reduced to

$$a_1 = (G_2\dot{G}_1 - G_1\dot{G}_2)/G^3 = \dot{\theta}/G. \tag{8}$$

In the adiabatic limit (1) $|a_1| = |\dot{\theta}/G| \ll 1$ $(\dot{\theta} = \partial\theta/\partial\tau)$, i.e., the population of the intermediate state $|1\rangle$ is close to zero all the time during the interaction with pulses. This also implies that the resonant absorption of the light pulses is weak (electromagnetically induced transparency) and the population is mainly distributed between the initial $|0\rangle$ and the final $|2\rangle$ states:

$$|a_0|^2 + |a_2|^2 \simeq 1. \tag{9}$$

Equality (9) reflects the fact that atoms are trapped in the CPT state: $a_{CPT} = (G_2/G)a_0 - (G_1/G)a_2 = a_0\cos\theta - a_2\sin\theta = 1$. This effect is responsible for the decrease in the resonant absorption of the propagating pulses. Also Raman coherence $\rho_{20} = a_0 a_2^*$ occurs:

$$\rho_{20} = -\frac{1}{2}\sin(2\theta) \quad \text{for} \quad \rho_{20} = -\frac{G_1 G_2}{G_1^2 + G_2^2}. \tag{10}$$

Obviously, the maximum coherence (in absolute value) $|\rho_{20}| = 1/2$ is reached when $\theta = \pi/4$ $(G_1^0 = G_2^0)$. Figure 2 shows the temporal behavior of the level populations $|a_{0,2}(\tau)|^2$, the atomic Raman coherence $|\rho_{20}(\tau)|$, and the mixing angle $\theta(\tau)$ for Gaussian pulses in an optically thin medium.

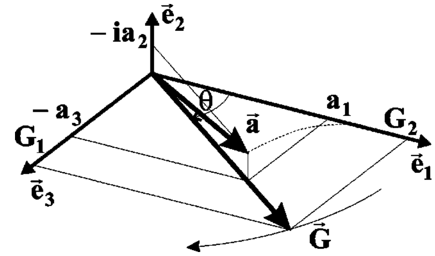

FIG. 3. The vector model of adiabatic interaction of two short pulses with a three-level Λ-type system.

The above results can be interpreted in terms of the three-dimensional vector model where vector variables $\vec{a} = (a_0, a_2, a_1)$ and $\vec{G} = (G_2, G_1, 0)$ (the torque vector) are introduced. Using these variables, we can rewrite Eq. (4) as

$$\dot{\vec{a}} = \vec{G} \times \vec{a}, \tag{11}$$

where the sign $\times$ means the vector product. The solution of Eq. (11) is the vector $\vec{a} = (G_2/G, -G_1/G, \dot{\theta}/G)$. Components of the vector $\vec{a}$ coincide with the adiabatic solution (6). Figure 3 illustrates the dynamics of vectors $\vec{G}$ and $\vec{a}$ in the three-dimensional vector model. The torque vector $\vec{G}$ moves in the $\vec{e}_1$-$\vec{e}_2$ plane, and vector $\vec{a}$ having a small angle with respect to vector $\vec{G}$ $(|\dot{\theta}/G| \ll 1)$ follows it. Thus one can see an absolute analogy with the adiabatic following in the case of a light pulse interacting with a two-level atom [27]. Such a simple picture can be observed only in optically thin media. In optically dense media, $G_{1,2}$ and hence θ become dependent on the z coordinate.

IV. SPATIAL EVOLUTION OF INTERACTING PULSES IN OPTICALLY DENSE MEDIA

A. General case: Unequal oscillator strengths ($K_1 \neq K_2$)

The condition $K_1 \neq K_2$ means that the probability of the $|0\rangle$-$|1\rangle$ transition is not equal to that of the $|2\rangle$-$|1\rangle$ transition. We note that in the ideal adiabatic limit $a_1 = 0$, and the pulses would not change their shape as they propagate in a medium that is optically thick for each of the pulses [see Eq. (5)]. However, this is not the case. The nonadiabatic correction has to be introduced for real situations, which results in induced dipole moments at the transitions $|1\rangle$-$|0\rangle$ and $|1\rangle$-$|2\rangle$, and in the change of both pulses traveling in the medium. In order to attribute this effect to propagation of the interacting pulses in an optically dense medium, it is necessary to solve Eqs. (4) and (5) in a self-consistent way.

Use Eqs. (7) and (8) to rewrite the field equations (5) in the form

$$\frac{\partial G_1}{\partial z} = -K_1 \frac{\dot{\theta}}{G}\cos\theta, \quad \frac{\partial G_2}{\partial z} = K_2 \frac{\dot{\theta}}{G}\sin\theta. \tag{12}$$

From Eq. (12), one can show that

$$K_2G_1^2(\tau,z)+K_1G_2^2(\tau,z)=K_2G_1^2(\tau,z=0)+K_1G_2^2(\tau,z=0), \tag{13}$$

i.e., $K_2G_1^2(\tau,z)+K_1G_2^2(\tau,z)$ does not depend on the z coordinate. Equation (13) describes the Manley-Raw relation, i.e., the law of conservation of the total energy density during propagation under CPT conditions.

Using the definitions of θ and G, we obtain the following expressions for $G_{1,2}(\tau,z)$:

$$G_1(\tau,z)=G(\tau,z)\sin\theta(\tau,z),$$

$$G_2(\tau,z)=G(\tau,z)\cos\theta(\tau,z). \tag{14}$$

Substitution of Eqs. (14) into the Manley-Raw relation gives the following expression for $G(\tau,z)$:

$$G^2(\tau,z)=G_0^2(\tau)\frac{K_2\sin^2[\theta_0(\tau)]+K_1\cos^2[\theta_0(\tau)]}{K_2\sin^2[\theta(\tau,z)]+K_1\cos^2[\theta(\tau,z)]}, \tag{15}$$

where $G_0^2(\tau)=G_1^2(\tau,0)+G_2^2(\tau,0)$ and $\theta_0(\tau)=\theta_0(\tau,0)$ are the functions at the medium entrance, $z=0$.

So the dynamics of level populations as well as the atomic Raman coherence and the evolution of the pulse shape are completely determined by the function $\theta(\tau,z)$ which depends on both the time τ and the coordinate z. Differentiating $\tan\theta=G_1/G_2$ with respect to z and using Eq. (12) we obtain the following equation for $\theta(\tau,z)$:

$$\frac{\partial\theta}{\partial\tau}+\frac{G^2(\tau,z)}{K(\theta)}\frac{\partial\theta}{\partial z}=0, \tag{16}$$

where $K[\theta(\tau,z)]=K_1\cos^2[\theta(\tau,z)]+K_2\sin^2[\theta(\tau,z)]$.

Equation (16) is similar to the equations describing nonlinear waves with the sharpening of the wave front during propagation [28]. The parameter $u=G^2/K$ can be treated as the "nonlinear" velocity. The nonlinear velocity can be described as $u(\tau,z)=A(\tau)/K^2[\theta(\tau,z)]$ where the first factor $A(\tau)=G_0^2(\tau)\{K_2\sin^2[(\theta_0(\tau)]+K_1\cos^2(\theta_0(\tau)]\}$ is independent of the z coordinate, and the second factor $K[\theta(\tau,z)]$ is maintained along a characteristic of Eq. (16) $\theta(\tau,z)=\text{const}$. This allows us to write down the characteristic curve equation in an obvious form:

$$z=\frac{1}{K^2(\theta_0)}\int_{\tau_0}^{\tau}A(\tau')d\tau'. \tag{17}$$

Here $\theta_0=\theta_0(\tau_0,0)$ is the function $\theta(z,\tau)$ at the medium entrance $z=0$, and τ_0 is the time at which the characteristic curve goes out of the medium boundary.

The solution for $\theta(\tau,z)$ has the form

$$\theta(\tau,z)=\theta_0(\tau_0,0). \tag{18}$$

Here τ_0 is to be determined from Eq. (17).

B. The case of equal oscillator strengths ($K_1=K_2$)

In the case of equal oscillator strengths $K_1=K_2\equiv K$ the $G(z,\tau)$ function is not subject to changes during propagation [$G(\tau,z)=G_0(\tau)$—the Manley-Raw relation for this case]. Therefore Eq. (16) substantially simplifies:

$$\frac{\partial\theta}{\partial\tau}+\frac{G_0^2(\tau)}{K}\frac{\partial\theta}{\partial z}=0. \tag{19}$$

The solution of Eq. (19) can be written in the following form:

$$\theta(\tau,z)=\theta_0(Z^{-1}(Z(\tau)-z),0), \tag{20}$$

where $Z(\tau)=K^{-1}\int_{-\infty}^{\tau}d\tau' G^2(0,\tau')$, and $Z^{-1}(\tau)$ is the inverse function of $Z(\tau)$.

It is not difficult to show that in this case $G=\sqrt{G_1^2(\tau,z)+G_2^2(\tau,z)}$ coincides with the definition of dressed field pulses [12,13]: $G_-=a_0G_2-a_2G_1$. Thus the pulses in our case can be identified as dressed field pulses (only at $K_1=K_2$). It is interesting to note the other combination $G_+=a_0G_1+a_2G_2\equiv 0$ (see also [12]). The concept of dressed field pulses cannot be applied to the case of $K_1\neq K_2$, but in both cases the Manley-Raw relation remains valid.

C. The adiabaticity criterion

The above results were obtained on the assumption that the adiabaticity criterion (1) (or $|\dot{\theta}/G|\ll 1$) remains valid during propagation of pulses. However, that is not necessarily the case. Therefore we investigate the adiabaticity condition taking account of propagation. Differentiating Eq. (18) with respect to τ, we can write the following expression for the adiabaticity criterion:

$$\frac{\dot{\theta}(\tau,z)}{G(\tau,z)}=\frac{\partial\theta_0}{\partial\tau_0}\frac{G(\tau,z)}{G_0^2(\tau_0)}\frac{K[\theta(\tau,z)]}{K[\theta_0(\tau_0)]}\times\left[1+\sin[2\theta_0(\tau_0)]\frac{2(K_2-K_1)z}{G_0^2(\tau_0)}\frac{\partial\theta_0}{\partial\tau_0}\right]^{-1}\ll 1. \tag{21}$$

As follows from Eq. (21), the adiabaticity condition is destroyed ($\dot{\theta}/G\rightarrow\infty$) when the factor in large square brackets tends to zero. Since $\sin[2\theta_0(\tau_0)]>0$ in the entire range of change of θ $(0\leqslant\theta\leqslant\pi/4)$, relation (21) is not fulfilled under the following conditions:

$$\frac{2(K_1-K_2)z}{G_0^2(\tau_0)}\frac{\partial\theta_0}{\partial\tau_0}\sin[2\theta_0(\tau_0)]=1,$$

$$(K_1-K_2)\frac{\partial\theta_0}{\partial\tau_0}>0. \tag{22}$$

Evidently, condition (22) is not satisfied at $K_1=K_2$, and the adiabaticity criterion holds throughout the propagation

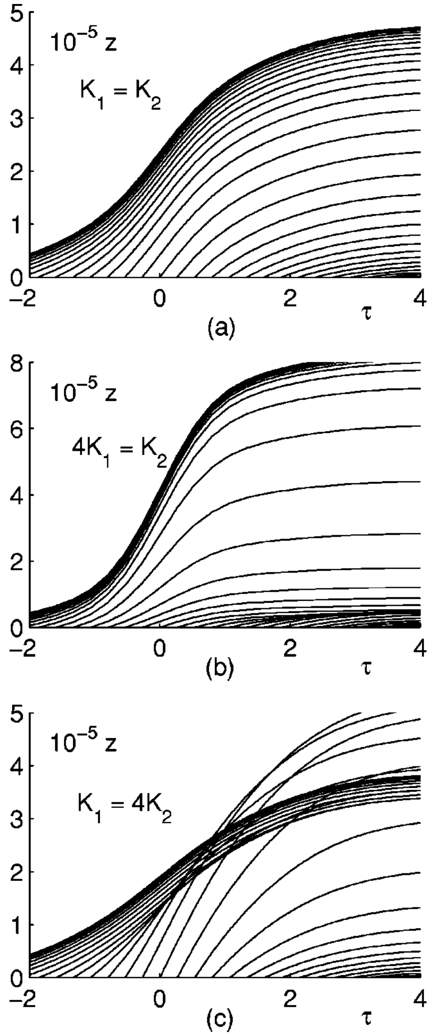

FIG. 4. The characteristic curves for Eq. (16): (a) $K_1/K_2=1$, (b) $K_1/K_2=0.25$, and (c) $K_1/K_2=4$.

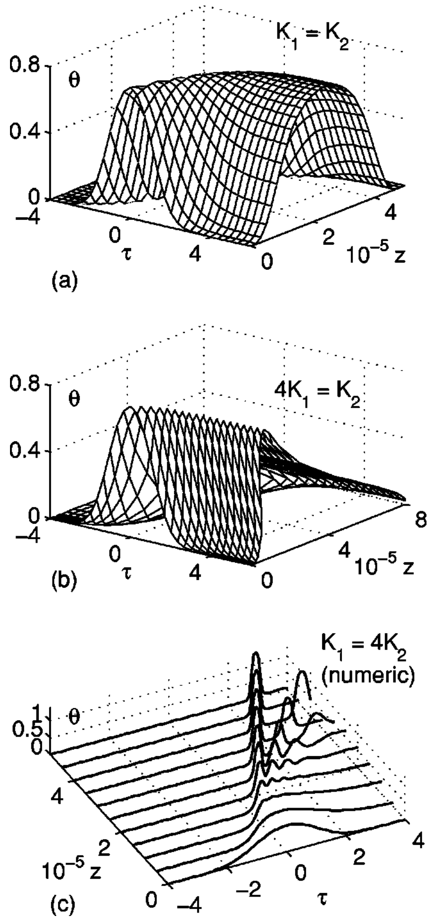

FIG. 5. The time evolution of the parameter θ for different relationships between K_1 and K_2 at different propagation lengths. (a) $K_1=K_2$, (b) $K_1/K_2=0.25$, and (c) $K_1/K_2=4$. $G^0_{1,2}T_1=20$, $T_2/T_1=3$. Here and in all the other figures the time τ is measured in units of the pulse duration T_1, and the propagation length z of pulses in the medium is measured in units of the length of linear absorption of the probe radiation determined in accordance with Beer's law. In (c) the numerical solution for the case $K_1/K_2=4$ is presented.

process. It should be mentioned that numerical analysis of Eq. (22) reveals that, generally speaking, there is a range of change of the $q=K_1/K_2$ parameter when the first condition in Eq. (22) is not satisfied either: $q_{min}<q<q_{max}$, $q_{min}<1$, $q_{max}>1$. The values q_{max} and q_{min} depend on the ratio $a=T_2/T_1$ and the shape of the pulses. For example, the q parameter for Gaussian pulses with $T_2/T_1=3$ may vary within the limit $0.40<q<1.35$, as shown by numerical simulation.

In this case for the thick medium the adiabaticity criterion has the form

$$\frac{\partial\theta_0}{\partial\tau_0}\frac{G(\tau,z)}{G_0^2(\tau_0)}\ll 1. \tag{23}$$

It can be readily shown that condition (23) for Gaussian pulses is satisfied when $T_2/T_1>\sqrt{3}$ and $G_2^0T_1\gg 1$ (compare with the case of the thin medium).

For Gaussian pulses ($T_2>T_1$) and the initial conditions $a_0(-\infty)=1$, $a_2(-\infty)=0$, we have $\dot{\theta}_0>0$ for $-\infty<\tau_0<0$. With $K_1>K_2$ ($q>q_{max}$) the adiabaticity criterion begins to break down at the leading edge: the mixing angle front becomes steeper. Condition (21) is destroyed at the trailing edge (where $\dot{\theta}_0<0$) when $K_1<K_2$ ($q<q_{min}$). Let us introduce a critical length z_c at which the adiabaticity condition (21) cannot be satisfied. Using Eq. (22), one can obtain the following simple estimation for z_c for the case $K_1\neq K_2$:

$$z_c\simeq\frac{G_0^2T_1}{2|K_1-K_2|}. \tag{24}$$

Let us now consider the experimental parameters. $N=10^{15}\ \text{cm}^{-3}$; $1/\lambda_{1,2}=10\,000,\ 20\,000\ \text{cm}^{-1}$; $1/\gamma_{1,2}=10,50$ ns are the relaxation times of levels $|1\rangle$ and $|2\rangle$, respectively; $T_1=0.1$ ns; $G^0_{1,2}T_1=20$; $a=T_2/T_1=3$; $fg_{10}=0.1$ is the oscillator strength of the probe transition. From Eq. (24) we obtain $z_c=10^5z_0\approx 2$ cm, where z_0 is the linear absorption length. This estimation agrees with the results presented in Figs. 5–7 below.

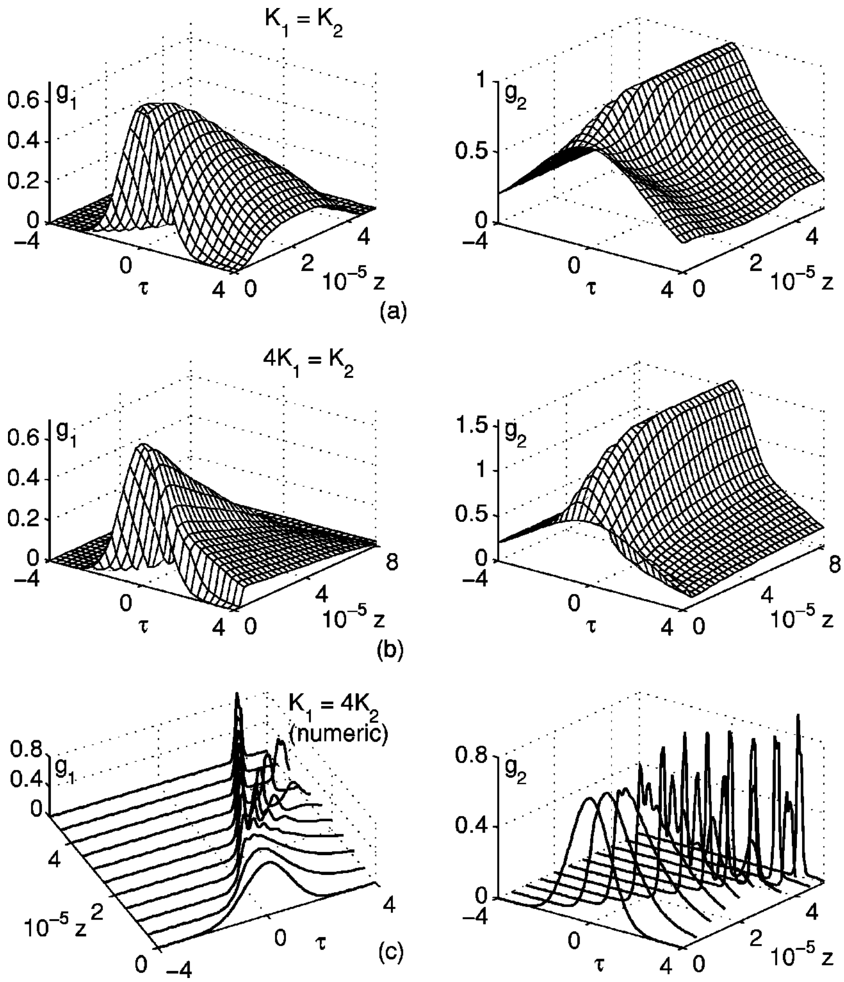

FIG. 6. The time evolution of the normalized Rabi frequencies $g_{1,2}=G_{1,2}/\sqrt{(G_1^0)^2+(G_2^0)^2}$ of the probe and coupling pulses for different relationships between K_1 and K_2 at different propagation lengths. (a) $K_1=K_2$, (b) $K_1/K_2=0.25$, and (c) $K_1/K_2=4$. $g_{1,2}^0=20$, $T_2/T_1=3$.

Using the characteristic equation (17) it is easy to find the area where the adiabaticity criterion breaks down. Characteristic curves for various values of $q=K_1/K_2$, $q=1$, 0.25, and 4, are shown in Fig. 4. The thickening of the characteristic curves means the sharpening of the mixing angle front at a certain medium depth. At the point of intersection [see Figs. 4(b) and 4(c)], $\dot{\theta}\to\infty$, condition (21) collapses. However, there are no such points in the case [see Fig. 4(a)] where $q_{min}<q<q_{max}$, i.e., the adiabaticity criterion (21) is maintained during propagation of pulses.

The above discussion is illustrated by Fig. 5 where the temporal behavior of the mixing angle θ is presented for $q=K_1/K_2=1,0.25,4$ and for different normalized propagation lengths. In Figs. 5(a) and 5(b) the analytical results are presented [formulas (18) and (20)]. Figure 5(c) shows the numerical solution for θ at $K_1>K_2$.

One can see that the evolution of the θ parameter at $K_1>K_2$ is different from that at $K_1<K_2$. At $K_1>K_2$ the adiabaticity condition fails for all values of z, beginning from the critical lengths z_c defined by Eq. (24). Here, the analytical theory does not apply at the very late stage of nonlinear wave propagation. In the case of $K_1<K_2$, nonadiabaticity develops at the trailing edge (the front becomes steeper at a certain propagation length), but it does not go deeper into the medium. A good agreement between the analytical and numerical solutions for θ at $K_1\leqslant K_2$ is observed over the entire propagation length. This leads us to conclude that the interaction adiabaticity is fairly sensitive to the ratio of the oscillator strengths of the transitions interacting with the pulses.

D. Discussion of results

The solutions obtained have been used to analyze the temporal dynamics and spatial behavior of propagating EIT pulses and the atomic coherence for various oscillator strength ratios. Figure 6 illustrates the temporal and spatial evolution of normalized Rabi frequencies of both pulses $g_{1,2}(\tau)=G_{1,2}/\sqrt{(G_1^0)^2+(G_2^0)^2}$ as they propagate inside an optically thick medium. The temporal evolution of pulses can be seen to depend on the ratio between the transition oscillator strengths. In the case of $K_1\leqslant K_2$ both pulses undergo reshaping as they propagate in the medium [Figs. 6(a) and 6(b)]. The probe pulse is gradually depleted and the coupling gets stronger. Note that the pulse shape at the initial stage of propagation shows very little change along the length of the medium, which may exceed the linear absorption length. Complete reemitting of the probe pulse into the coupling one during propagation is possible. Using Eq. (17) one can obtain the following expression for the maximal distance z_m for which the probe pulse propagates into the medium:

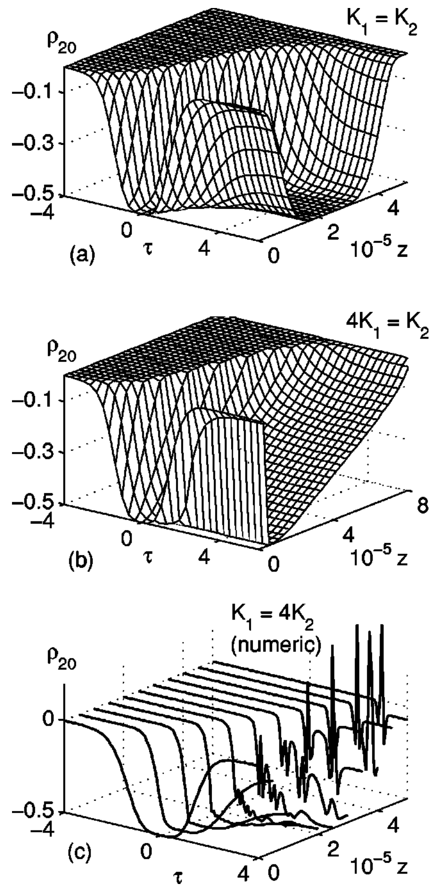

FIG. 7. The time evolution of the atomic Raman coherence for different relationships between K_1 and K_2 at different propagation lengths. (a) $K_1=K_2$, (b) $K_1/K_2=0.25$, and (c) $K_1/K_2=4$. $G_{1,2}^0 T_1 =20$, $T_2/T_1=3$.

$$z_m=\frac{1}{K^2(\theta_0(-\infty))}\int_{-\infty}^{\infty}A(\tau)d\tau. \tag{25}$$

For Gaussian pulses we have

$$z_m=\sqrt{\frac{\pi}{2\ln 2}}(G_2^0)^2T_1\frac{K_2(G_1^0/G_2^0)^2+K_1a}{K_1^2}. \tag{26}$$

Here $a=T_2/T_1$.

For the same parameters as in the previous subsection, we have $z_m=4.8\times10^5 z_0\approx 9$ cm for $K_1/K_2=1$ and $z_m =8.4\times10^5 z_0\approx 16$ cm for $K_1/K_2=1/4$. These values agree with the results shown in here.

An interesting feature of the spatial distribution of the probe pulse is illustrated in Figs. 6(a,b): in some areas of the medium, the field in the tail of the pulse is different from zero. This is believed to be the result of the spatial compression of the probe caused by the slowing down of the group velocity of the probe pulse [26].

In the case of $K_1>K_2$, the adiabaticity condition is maintained over the z_c range, which can also be much longer than the length of the linear absorption. The leading edge of the probe pulse undergoes gradual depletion and the pulse amplitudes display only small changes in that range. Outside that range, the pulse splits into several peaks. This occurs due to the nonadiabaticity of interaction. [see Fig. 6(c) where numerical simulations are presented for $g_{1,2}(\tau)$. Here the first three curves correspond to the adiabatic interaction.]

The pulse evolution, described above, is determined by the spatial and temporal behavior of the atomic Raman coherence ρ_{20} shown in Fig. 7 (see also [18]). Figures 7(a,b) reveal an unusual spatial and temporal behavior of the atomic coherence, which we interpret as the slowing down, stopping, and localization of the atomic coherence in the medium. The probe pulse is transferred into and stored in the collective atomic excitation under the control of the coupling. One can say that a phase grating is created in the atomic medium. The phase grating is preserved throughout the entire period of relaxation of the atomic coherence. During that period of time, the information stored in the atomic excitations can be transferred back to the radiation using another coupling pulse of the same or of a different frequency.

We find these effects to be similar to the ones predicted and demonstrated in [9,10,26], but for some differences as indicated below. In our case, both the coupling pulse and the probe pulse are strong. Unlike [26], we used boundary conditions for the pulse envelopes yielding a time distribution of pulses at the medium boundary $z=0$. We believe this condition is more natural than the one used in [26] where the authors use the probe pulse distribution in the medium at a fixed time as the initial condition. Also, they do not take into consideration evolution of the coupling pulse. The effect takes place in the case $K_1\leqslant K_2$ and is not observed in the case of $K_1>K_2$.

V. CONCLUSION

The propagation of two short overlapping pulses with durations $T_2>T_1$ in optically thick three-level media under CPT conditions has been studied for the general case of unequal transition oscillator strengths. An analytical solution has been obtained for the set of reduced wave equations under the adiabatic following condition. Also it has been shown how the spatial evolution of pulses depends on the oscillator strength ratio.

The condition of adiabaticity provided at the medium entrance preserves for any value of propagation lengths if $K_1 \leqslant K_2$ $(q<q_{max})$ and breaks down at $K_1>K_2$ $(q>q_{max})$. In the range $q<q_{max}$, the probe pulse is completely depleted and reemitted into the coupling pulse during propagation. This is not possible in the case of $q>q_{max}$. It has been established that, to provide for the adiabaticity condition in an optically thin medium, the restriction $T_2/T_1>\sqrt{2}$ has to be ensured, whereas in a thick medium $T_2/T_1>\sqrt{3}$.

We have also studied the spatial behavior of the atomic coherence ρ_{20}, which plays a significant role, for example, in nonlinear mixing processes. It has been found that a strong coherence can be maintained over a length equal to several hundreds of thousand of one-photon absorption lengths during propagation. The effect of localization of the atomic coherence is demonstrated.

[1] S. E. Harris, Phys. Today **50**, 36 (1997).
[2] S. G. Rautian and A. M. Shalagin, *Kinetic Problem of Nonlinear Spectroscopy* (North-Holland, Amsterdam, 1991); A. K. Popov, *Vvedenie v Nelineinuyu Spectroscopiyu* (Nauka, Novosibirsk, 1983).
[3] B. D. Agap'ev, M. B. Gornyi, B. G. Matisov, and Yu. V. Rozhdestvensky, Usp. Fiz. Nauk **163**, 1 (1993).
[4] E. Arimondo, in *Progress in Optics* edited by E. Wolf (Elsevier, Amsterdam, 1996), Vol. 35, p. 257.
[5] K. Bergman, H. Theuer, and B. W. Shore, Rev. Mod. Phys. **70**, 1003 (1998).
[6] S. E. Harris and Y. Yamamoto, Phys. Rev. Lett. **81**, 3611 (1998).
[7] L. V. Hau, S. E. Harris, Z. Dutton, and C. H. Behroozi, Nature (London) **397**, 594 (1999).
[8] M. M. Kash, *et al.*, Phys. Rev. Lett. **82**, 5229 (1999).
[9] D. F. Phillips, A. Fleischhauer, A. Mair, R. L. Walsworth, and M. D. Lukin, Phys. Rev. Lett. **86**, 783 (2001).
[10] C. Liu, Z. Dutton, C. H. Behroozi, and L. V. Hau, Nature (London) **409**, 490 (2001).
[11] S. E. Harris, Phys. Rev. Lett. **72**, 52 (1994).
[12] J. H. Eberly, M. L. Pons, and H. R. Haq, Phys. Rev. Lett. **72**, 56 (1994).
[13] J. H. Eberly, Quantum Semiclassic. Opt. **7**, 373 (1995).
[14] J. H. Eberly, A. Rahman, and R. Grobe, Phys. Rev. Lett. **76**, 3687 (1996).
[15] R. Grobe, F. T. Hioe, and J. H. Eberly, Phys. Rev. Lett. **73**, 3183 (1994).
[16] M. Fleischhauer and A. S. Manka, Phys. Rev. A **54**, 794 (1996).
[17] V. G. Arkhipkin, D. V. Manushkin, and V. P. Timofeev, Quantum Electron. **28**, 1055 (1998).
[18] V. G. Arkhipkin and I. V. Timofeev, Proc. SPIE **4002**, 45 (1999).
[19] A. Kasapi, M. Jain, G. Y. Yin, and S. E. Harris, Phys. Rev. Lett. **74**, 2447 (1995).
[20] G. G. Grigoryan and Y. T. Pashayan, Proc. SPIE **4060**, 21 (1999).
[21] F. T. Hioe and R. Grobe, Phys. Rev. Lett. **73**, 2559 (1994).
[22] M. Jain, X. Hia, G. Y. Yin, A. J. Merriam, and S. E. Harris, Phys. Rev. Lett. **77**, 4326 (1996); A. J. Merriam, S. J. Sharpe, H. Xia, D. Manuszak, G. Y. Yin, and S. E. Harris, Opt. Lett. **24**, 625 (1999).
[23] V. G. Arkhipkin, D. V. Manushkin, S. A. Myslivets, and A. K. Popov, Quantum Electron. **28**, 637 (1998).
[24] J. R. Kuklinski, U. Gaubats, F. T. Hioe, and K. Bergman, Phys. Rev. A **40**, 6471 (1989).
[25] U. Gaubats, P. Rudecki, S. Schiemann, and K. Bergman, J. Chem. Phys. **92**, 5363 (1990).
[26] M. Fleischhauer and M. D. Lukin, Phys. Rev. Lett. **84**, 5094 (2000).
[27] L. Allen and J. Eberly, *Optical Resonance and Two-Level Atoms* (Wiley, New York, 1975).
[28] R. Z. Sagdeev, D. A. Usikov, and G. M. Zaslavsky, *Nonlinear Physics* (Harwood, Chur, Switzerland, 1988).